populations (*9–12*). Since the littoral macrophage or Kupffer cell appears to be important in the pathogenesis of murine viral hepatitis (*21*), the action of glucan against MHV-A59 may be due to its ability to increase hepatic macrophage number (*3*) and function (*2*) and thus prevent initial viral replication, alter subsequent generations of viral progeny, or eliminate the virus. The present study supports the concept that the pathogenesis of viral infections is determined, in part, by macrophage-virus interactions (*13, 21–24*).

Murine infections with MHV 1 have been reported to result in primary involvement of the Kupffer cells (*21, 22*) and a subsequent lysis of these cells and release of virus particles (*22*). This impairment or destruction of liver macrophages results in a decrease of phagocytic function, with the degree of dysfunction related to the virulence of the virus (*23*). Previous studies also demonstrated that "activation" of peritoneal macrophages by a variety of immunomodulators resulted in increased antiviral and antitumor activity (*24*). Our observations with glucan are in agreement with these findings.

The phagocytic function of macrophages was enhanced when the mice were treated with glucan before being challenged with MHV-A59. Gledhill *et al.* (*23*) reported that MHV 3, another virulent murine hepatitis virus, causes a significant reduction in the intravascular clearance of colloidal carbon during the incubation period of the virus. This observation is in agreement with our data regarding the macrophage-suppressive activity of MHV-A59. Whether the decreased clearance of the RE lipid emulsion is due to impairment or destruction of Kupffer cells remains to be ascertained.

Histopathological examination of the liver on day 4 revealed that pretreating mice with glucan inhibited the viral destruction of hepatic tissue. Although some liver necrosis developed, the primary histological feature was the typical glucan-induced granulomatosis (*3*).

Since glucan has already been reported to have antitumor, antifungal, and antibacterial properties, it is apparent that this polyglucose is an immunotherapeutic agent with broad applications. Whether glucan can alter the course of human viral hepatitis remains to be determined.

DAVID L. WILLIAMS
NICHOLAS R. DI LUZIO
Department of Physiology, Tulane University School of Medicine, New Orleans, Louisiana 70112

References and Notes

1. W. R. Wooles and N. R. Di Luzio, *Science* **142**, 1078 (1963).
2. _____, *J. Reticuloendothel. Soc.* **1**, 160 (1964).
3. C. T. Ashworth, N. R. Di Luzio, S. J. Riggi, *Exp. Mol. Pathol. Suppl.* **1**, 83 (1963).
4. W. Browder, R. McNamee, N. R. Di Luzio, *Surg. Forum* **28**, 171 (1977).
5. N. R. Di Luzio, R. McNamee, W. I. Browder, D. L. Williams, *Cancer Treat. Rep.* **62** (No. 11), 1857 (1978).
6. P. W. A. Mansell *et al.*, *J. Natl. Cancer Inst.* **54**, 571 (1975).
7. P. W. A. Mansell, N. R. Di Luzio, R. McNamee, G. Rowden, J. W. Proctor, *Ann. N.Y. Acad. Sci.* **277**, 20 (1976).
8. L. Israel and R. Edelstein, in *Immune Modulation and Control of Neoplasia by Adjuvant Therapy*, M. A. Chirigos, Ed. (Raven, New York, 1978), vol. 7, pp. 249–254.
9. N. R. Di Luzio and D. L. Williams, *Infect. Immun.* **20**, 804 (1978).
10. D. L. Williams, J. A. Cook, E. O. Hoffman, N. R. Di Luzio, *J. Reticuloendothel. Soc.* **23**, 479 (1978).
11. M. Song and N. R. Di Luzio, in *Lysosomes in Biology and Pathology*, P. J. Jacques and I. B. Shaw, Eds. (North-Holland, Amsterdam, 1979), vol. 6, pp. 533–547.
12. J. A. Reynolds, M. D. Kastello, D. G. Harrington, C. L. Crabbes, C. J. Peters, J. V. Jemski, G. H. Scott, N. R. Di Luzio, *Infec. Immun.*, in press.
13. S. C. Mogensen, *Microbiol. Rev.* **43**, 1 (1979).
14. W. Z. Hassid, M. A. Joslyn, R. M. McCready, *J. Am. Chem. Soc.* **63**, 295 (1941).
15. N. R. Di Luzio, J. C. Pisano, T. M. Saba, *J. Reticuloendothel. Soc.* **7**, 731 (1970).
16. P. L. Kokoshis, D. L. Williams, J. A. Cook, N. R. Di Luzio, *Science* **199**, 1340 (1978).
17. P. L. Kokoshis and N. R. Di Luzio, *J. Reticuloendothel. Soc.* **25**, 85 (1979).
18. M. Glovsky, N. R. Di Luzio, A. Alenty, L. Ghekiere, *ibid.* **20**, 54 (1976) (abstract).
19. C. Burgaleta and D. W. Golde, *Cancer Res.* **37**, 1734 (1977).
20. M. Chirigos and C. Neumann, personal communication.
21. B. Reubner and K. Miyai, *Am. J. Pathol.* **40**, 425 (1962).
22. F. B. Bang and A. Warwick, *Virology* **9**, 715 (1959).
23. A. W. Gledhill, D. L. J. Bilbey, J. S. Niven, *Br. J. Exp. Pathol.* **46**, 433 (1965).
24. P. S. Morahan, L. A. Glasgow, J. L. Crane, Jr., E. R. Kern, *Cell. Immunol.* **28**, 404 (1977).
25. Supported in part by the MECO Cancer Research Fund of New Orleans, American Cancer Society grant CA 1-3745, National Institute on Alcohol Abuse and Alcoholism grant AA 00309, and NCI grant CA 24326-01.

19 November 1979

Bronchial Bifurcations and Respiratory Mass Transport

Abstract. *A new transport mechanism explains the importance of the shape of bronchial bifurcations in the transfer of gases and particles between the atmosphere and the alveoli. Photographs of flow visualization experiments illustrate the effect in models of bronchial branching. The mechanism provides a means of nondiffusional transport that helps to explain normal respiratory exchange of gases as well as successful ventilation with very low tidal volumes, as in some lung diseases and in the high-frequency panting of dogs.*

Measurements in vivo of purely convective aerosol and gas movement through the bronchial tree have shown that, during each breath cycle, 10 to 25 percent of the inspired tidal volume is exchanged with the functional residual volume (*1–5*). A new mechanism based on the different velocity profiles generated at the bronchial bifurcations during inspiration and expiration explains this exchange as a well-ordered consequence of lung design. Furthermore, the way in which the exchange occurs suggests that this is an important factor in the transport of particles and in the efficient transport of gases between the atmosphere and the alveoli deep in the lung.

The bulk exchange mechanism induced by the lung airways depends on the fact that velocity profiles—that is, intra-airway flow patterns—are different during inspiration and expiration. A hypothetical example with two different velocity profiles in a single tube serves to illustrate the effect. Consider a tracer aerosol (Fig. 1), whose particles have a negligible coefficient of diffusion and negligible settling due to gravity, in-

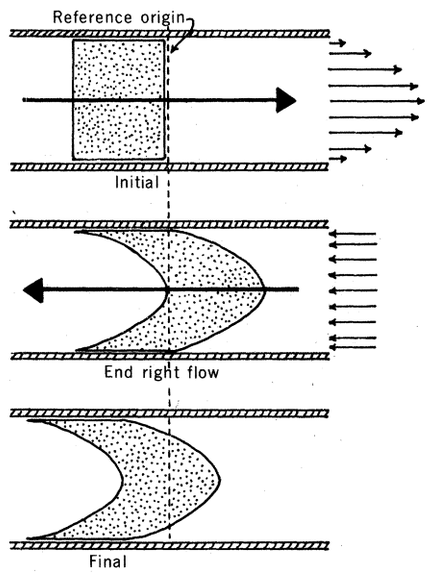

Fig. 1. Cross-sectional illustration of the convective exchange mechanism within a single tube. The position and shape of a tracer aerosol plug are shown at three times in a single flow cycle: initially, at the end of flow to the right and after an equal volume of flow to the left (final). Velocity profiles governing right and left flow are also shown. Net deformation of the fluid volume containing tracer aerosol results in an exchange of fluid across the fixed reference origin. At the end of the cycle the total net flow in the tube is zero, but aerosol particles near the center of the tube have a net movement to the right and those near the wall have a net movement to the left.

0036-8075/80/0404-0069$00.50/0

troduced as a cylindrical plug in an infinitely long, straight tube. The position of the right end of the plug in the tube is labeled the reference origin. An oscillating flow cycle is initiated with flow to the right. During this flow, the velocity profile is parabolic. The aerosol plug in its motion to the right is reshaped by the velocity variations across the tube; the original cylindrical shape is transformed to a paraboloid front. The flow is stopped and the same total volume flows back to the left. However, during the return flow a different velocity profile is imposed. For the sake of simplicity, we choose a flat, or uniform, velocity profile. This velocity profile does not result in any further deformation of the tracer aerosol; every particle is transported an equal distance to the left. These two different velocity profiles result in a net deformation of the volume of fluid containing the tracer aerosol. This change in shape reflects net movement to the right for aerosol particles near the center of the tube and net movement to the left for particles near the tube wall. A comparison of the initial and final particle positions shows that although the total flow is zero, there is a bulk exchange of aerosol across the reference origin. Calculations for this example show that during one flow cycle, 25 percent of the tidal volume is transferred to the right of the reference origin in the center of the tube, and an equal volume near the tube walls is transferred to the left.

The necessary condition for volume transfer to occur is variation between the velocity profiles of inspiration and expiration. Velocity profiles have been measured for steady one-way flow through models and casts of a single bronchial bifurcation (*6–9*). The expiratory profile is in general more uniform (flatter) across the tube than the corresponding inspiratory profile. The peaked nature of the inspiratory profile is maintained over a wide range of flow rates (*10*). A calculation based on differences between representative profiles of inspiration and expiration reported in the literature predicts, for one flow cycle through a single bifurcation, a net deformation of the tidal flow resulting in a volume exchange approximately equal to 5 percent of the tidal flow.

To observe the deforming effect of velocity profiles generated in flow oscillation through a single bifurcation, a flow visualization experiment was designed. A model, geometrically similar to a bronchial bifurcation, was built of clear Plexiglas tubing with branch angle 70° and inside diameter 3.5 cm. The model was filled with glycerin (kinematic viscosity ≈ 0.8 cm²/sec) and the flow oscillated at a fixed frequency and displacement volume by a sinusoidal pump. The displacement volume and frequency were chosen such that dynamic similarity was established between the liquid behavior in the model and convective air movement in the lung. Net flow movement was recorded by photographing the motion of a plug of neutrally buoyant, nondiffusing, 40-μm white beads at the middle of the inspiratory phase of each flow cycle. Figure 2, a and b, shows single-frame enlargements of the film record of one experiment. These photographs show net movement of the beads to the right and to the left from their initial position. When they are seen in the context of the other film frames, it is evident that each cycle of forward and reverse flow results in a net deformation very similar to that of the hypothetical single-tube example. The beads bowed out to the right in the two downstream tubes originated in the center of the plug, and the beads that have moved to the left were originally near the sides of the tube. With a reference origin chosen as in the hypothetical example above (the right end of the initial bead plug), analysis of the photographs shows that a deformation equivalent to a bulk exchange of approximately 5 percent of the tidal volume has occurred for each flow cycle.

The flow visualizations of net bead movement show that the branching geometry of the model creates velocity profiles sufficiently different to cause a deformation in an intially referenced portion of the tidal flow. The difference between velocity profiles is produced by inertial and frictional forces resulting from changes in the shape of the surfaces surrounding the fluid in its flow forward and back. Dynamic similarity between the flow in the model and the flow in the bronchial tree is determined by matching the Reynolds number, Re, and a dimensionless frequency parameter, α. By

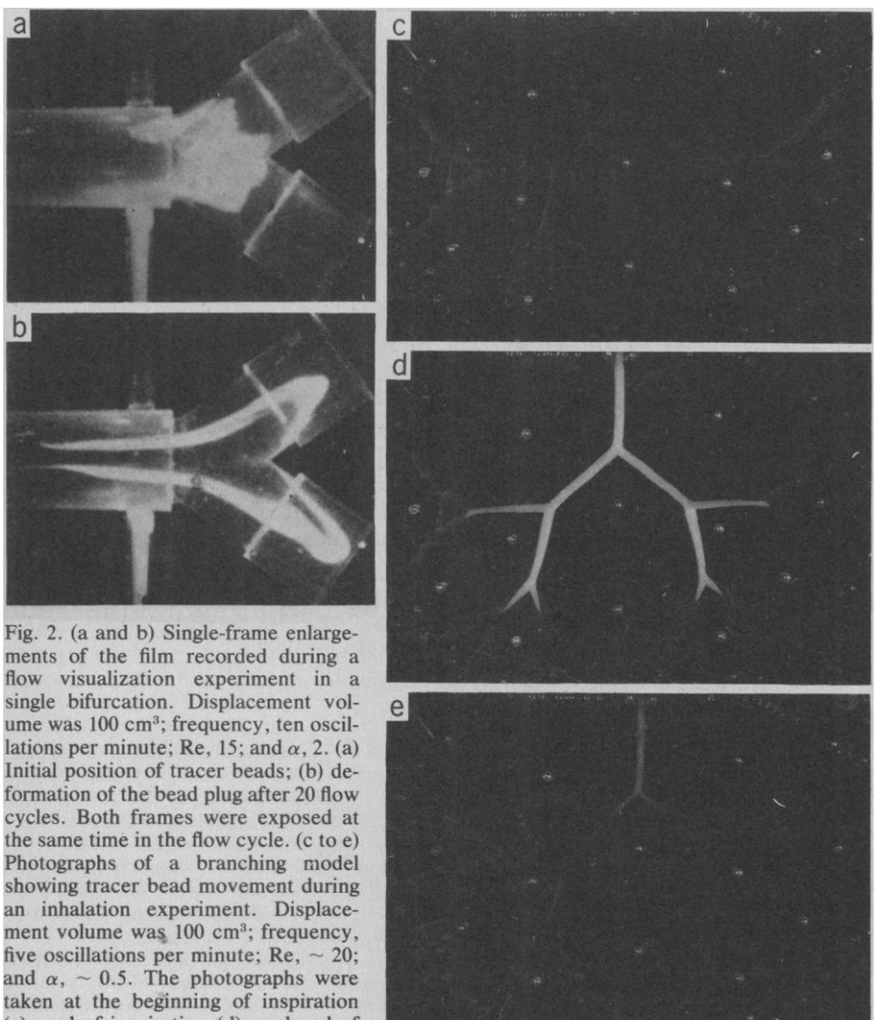

Fig. 2. (a and b) Single-frame enlargements of the film recorded during a flow visualization experiment in a single bifurcation. Displacement volume was 100 cm³; frequency, ten oscillations per minute; Re, 15; and α, 2. (a) Initial position of tracer beads; (b) deformation of the bead plug after 20 flow cycles. Both frames were exposed at the same time in the flow cycle. (c to e) Photographs of a branching model showing tracer bead movement during an inhalation experiment. Displacement volume was 100 cm³; frequency, five oscillations per minute; Re, ~ 20; and α, ~ 0.5. The photographs were taken at the beginning of inspiration (c), end of inspiration (d), and end of expiration (e) for one flow cycle. A residual amount of the inspired bead volume is shown trapped in the model at the end of the expiration.

choosing appropriate values of displacement volume and pumping frequency, Re and α were matched for normal breathing in regions of the bronchial tree between generations 7 and 15. These flow visualization experiments were thus relevant to the middle bronchial region, but any flow oscillating within a geometry different in the forward and reverse directions would experience a similar net internal deformation and consequent bulk exchange across an appropriate reference origin.

An enhancement of this effect would be expected for a multiple-branching geometry. An oscillating flow would encounter several bifurcations in series, each of which would create local velocity profile differences. Since the bifurcations all have the same orientation with respect to the flow—that is, flow splitting during inspiration—a cumulative net deformation greater than the effect of a single bifurcation would be expected.

This enhancement by serial bifurcations has been observed in aerosol inhalation experiments in man. In experiments with a 200-cm^3 bolus of tracer aerosol injected at different times during the inspiratory flow, Muir *et al.* (*11*) noted that the spreading of the bolus within the expired volume increased with the number of bifurcations the bolus had encountered. This increase in the volume containing the expired bolus is a direct measure of bolus deformation and consequent net movement across the reference points of the beginning and end of the inspired bolus.

It is well established that during a single normal breathing cycle, a bulk nondiffusive exchange of tidal air with the functional residual volume occurs (*1–5*). In these studies tracer aerosol was used in the inspired tidal volume and the cumulative aerosol return was measured at the mouth during expiration. The experimental results indicate that 10 to 25 percent of the tidal volume is an upper limit to the volume that may be transferred by a convective exchange mechanism during respiration. However, if the exchange process occurred in a well-ordered and cumulative fashion, the total effect over many breathing cycles would be significant.

To observe the net movement of tidal air in this type of inhalation experiment, another flow visualization experiment was designed. A multiple branch model with five generations was routed out of two 1.27-cm-thick Plexiglas sheets. These sheets were clamped together and the resulting internal network of tubes (inner diameter, 1.27 cm) was filled with clear glycerin (see Fig. 2, c to e) and ventilated by a system of tubes connecting the last generation to a sinusoidal pump. A 100-cm^3 tidal volume of glycerin containing white tracer beads with negligible gravitational settling and coefficient of diffusion was inspired into the model (Fig. 2d). The same tidal volume was then expired at the same breathing rate (five breaths per minute). Figure 2e shows the position of the tidal volume remaining in the model at the end of this single cycle. The time-averaged Reynolds number was 20 and the dimensionless frequency α was approximately 0.5, making the model dynamically similar to airflow behavior between generations 10 and 15.

Figure 2, c to e, shows that not only does a significant portion of the tidal volume remain beyond the model entrance, but, more important, its position at the end of the cycle dictates that it must precede the next inspired tidal volume into the model. The next tidal volume transports the newly exchanged portion of the previous tidal volume deeper into the model, and so on, in a similar well-ordered exchange that eventually fills the entire model. The total effect of a repetitive cycling of flow in and out of a multiple-branching geometry is a net forward flow, spanning several cycles, in the center of the tubes, and a balancing net backward flow near the tube walls. Thus, measured at the same time in each flow cycle, the total net volume flow is zero; however, internal circulation occurs to balance the variations in local flow deformations.

A similar phenomenon will also occur within the bronchial tree structure. The only requirement is a change, during inspiration and expiration, in the surrounding wall surfaces seen by the flow. No matter how asymmetric the structure, each splitting of the gas flow during inspiration and rejoining during expiration will generate different local velocity profiles. The magnitude of this difference will determine the extent of the local tidal volume deformation, and the accumulation of these deformations will result in a portion of the tidal volume remaining within the lung airways after normal exhalation. This exchange mechanism results in a net transfer of tidal air into the reservoir of the respiratory "dead space" and subsequently transports it from this reservoir ahead of the next inspired tidal volume deeper into the lung. Every net forward transfer of gas is continually balanced by a net backward transfer. A fraction of the exchange from the initial tidal volume continues to advance distally until a point in the lung structure is reached where the velocity profiles are no longer significantly different during the inspiratory and expiratory phases of flow.

For gases, molecular diffusion will affect transport in addition to the convective mechanism based on velocity profile differences. However, in regions of the bronchial tree where the ratio of bulk mass transfer to diffusive mass transfer—that is, the Peclet number—is large, the convective mechanism will predominate. Large Peclet numbers occur in the upper airways for normal breathing and deeper in the bronchial tree for high-frequency ventilation.

A bulk exchange rate of only 15 percent between tidal air and functional residual volume transfers more than enough oxygen to supply the basal metabolic needs from the atmosphere to the lung's interior. The convective gas exchange mechanism that we have described plays a major role in the initial exchange between atmosphere and lung interior and the convective delivery of gas to regions of the lung where diffusion can be utilized effectively. It suggests a design function for bronchial structure and gives new meaning to the respiratory dead space. In addition, it provides an explanation for successful ventilation with very low tidal volumes, as in some lung diseases (*12*) and the high-frequency panting of dogs (*13*).

F. R. HASELTON
P. W. SCHERER
Department of Bioengineering, University of Pennsylvania, Philadelphia 19104

References and Notes

1. B. Altshuler, E. D. Palmes, L. Yarmus, N. Nelson, *J. Appl. Physiol.* **14**, 321 (1959).
2. D. C. F. Muir, *ibid.* **23**, 210 (1967).
3. C. N. Davies, J. Heyder, M. C. Subba Ramu, *ibid.* **32**, 591 (1972).
4. D. B. Taulbee, C. P. Yu, J. Heyder, *J. Appl. Physiol. Respir. Environ. Exercise Physiol.* **44**, 803 (1978).
5. C. N. Davies, *J. Appl. Physiol.* **32**, 601 (1972).
6. T. J. Pedley, *Annu. Rev. Fluid Mech.* **9**, 229 (1977).
7. R. C. Schroter and M. F. Sudlow, *Respir. Physiol.* **7**, 341 (1969).
8. R. M. Schreck and L. F. Mockros, AIAA paper 70-788, delivered at the 3rd Fluid and Plasma Dynamics Conference, Los Angeles, 29 June to 1 July 1970.
9. D. E. Olson, L. D. Iliff, M. F. Sudlow, *Bull. Physio-Pathol. Respir.* **8**, 391 (1972).
10. R. Brech and B. J. Bellhouse, *Cardiovasc. Res.* **7**, 593 (1973).
11. D. C. F. Muir, K. Sweetland, R. G. Love, in *Inhaled Particles III: Proceedings*, W. H. Walton, Ed. (Pergamon, Elmsford, N.Y., 1971), pp. 81–90.
12. W. A. Briscoe, R. E. Forster, J. H. Comroe, Jr., *J. Appl. Physiol.* **7**, 27 (1954).
13. D. J. Bohn, W. Butler, A. B. Froese, A. C. Bryan, *Fed. Proc. Fed. Am. Soc. Exp. Biol.* **38**, 951 (1979).
14. Supported by grant HL20105 from the National Heart, Lung, and Blood Institute.

16 March 1979; revised 16 November 1979